JOURNAL OF MATERIALS SCIENCE **38** (2003) 1579–1584

The second phases in a burn resistant stable beta titanium alloy—Ti40

Y. Q. ZHAO, H. L. QU, K. Y. ZHU, H. WU, L. ZHOU
Northwest Institute for Nonferrous Metal Research, P.O. Box 51 Xi'an, Shaanxi 710016, People's Republic of China

The second phases in Ti40 (Ti25V-15Cr-0.2Si) burn resistant titanium alloy are studied. The higher solution temperature, the more second phases in Ti40 alloy. There are not second phases if the solution temperature is below 850°C, while there are rod-like α and little Ti_5Si_3 phases if temperature is over 850°C. α, Ti_5Si_3 and oblique α'' phases emerge after Ti40 solution at 910°C followed by aging at 600°C, while only Ti_5Si_3 phases emerge after solution at 860°C followed by aging at 600°C. The effect of the second phases on properties at RT are not obvious. There are different shapes of α and Ti_5Si_3 precipitates after Ti40 alloy exposure at 540°C for 100 h, which decreases the thermal stability.

1. Introduction

Titanium and its alloys have been extensively used in modern advanced aero-engines because of their excellent comprehensive properties, such as the F119 engine that powers the F22 USAF jet fighter consumes 39% titanium [1–3], which leads to great increase of the thrust-to-weight ratio. However, in order to reduce weight and increase the whole structural efficiency, the advanced engines not only need the excellent conventional comprehensive properties of titanium alloys, but also require their good burn resistance in order to replace Ni-based superalloys use in some crucial parts. There were different kinds of burn resistant titanium alloys since the early 1990s, such as Alloy C (Ti-35V-15Cr) [1–4] developed in USA, BTT-1 and BTT-3 invented in Russia [5], Ti-25V-15Cr-xAl-xC [6–8] developed in UK and Ti40 (Ti-25V-15Cr-0.2Si) [9–13] and Ti14 (Ti-1Al-13Cu-0.2Si) [14, 15] developed in China. The comprehensive properties of Ti-V-Cr burn resistant alloys are better than that of Ti-Al-Cu alloys [16], and Alloy C has been used in some practical components of the F119 engine [1–4] which was drawn attentions. Both Alloy C and Ti40 are stable beta type burn resistant alloys. There is no addition of minor alloying elemental Si in Alloy C, and small amount of precipitates of second α phases emerged after it exposed at 540°C for a long time [17]. Ti-25V-15Cr-xAl-xC does not contain Si either, and there will be precipitates of TiC and Ti_3Al phases after its exposure over 400°C for a long time [6–8]. Generally, alloying elemental Si is added to alpha alloys in order to improve the creep resistance. This element is also added to some typical $\alpha + \beta$ titanium alloys, such as Ti62222s (Ti-6Al-2Sn-2Zr-2Mo-2Cr-0.2Si) and BT3-1 (Ti-6Al-2.5Mo-1.5Cr-0.5Fe-0.35Si). This element may precipitate in the form of a (Ti, Zr)$_x$Si$_5$ phase after a prolonged annealing treatment. However Si is seldom added to beta titanium alloys except for metastable β21S (Ti-15Mo-3Al-2.7Nb-0.25 Si). Although Si is rarely added to β alloys, some people used it in metastable β alloys on purpose (such as β_{cez}) and studied its existing forms and its influence [18]. The silicide phase is nearly the same in all alloys. Only three elements are present in this phase: titanium, zirconium and silicon. Its space group was identified as P6/mmm in metastable beta alloys and P62m in alpha alloys, but it should be said that P6/mmm and P62m are very similar [18]. A beta matrix with a uniform distribution of silicides exhibits a ductile transgranular failure and a very good tensile ductiliy. On the opposite, a continuous grain boundary silicide precipitation results in intergranular fracture and a low elongation to rupture [18]. At present, the application of stable beta alloys are very limited and Si is seldom added, of course. This present paper is to study the form, distribution of second phase in stable Ti40 alloy with addition of Si and its influence on properties.

2. Experimental procedures

A 5-kg Ti40 alloy ingot (90 mm in diameter and 125 mm in height) was used in this study. Its chemical composition was Ti-24.6V-14.6Cr-0.33Si-0.15O. The ingot breakdown was conducted through two ways: one is by conventional forging to pancake of 25 mm-thickness (A); another is by isothermal forging to the same thickness pancake (B). Their tensile properties at RT and thermal stability were examined after different heat treatments. JSM-5800 scanning electron microscopy (SEM) was used for tensile fractographs, H-600 transmission electron microscopy (TEM) was used for microstructures.

3. Results and discussions

3.1. TEM observation

3.1.1. Solution treatment

Only β phase can be observed by means of optical microscopy (OM) under all kinds of heat treatment conditions.

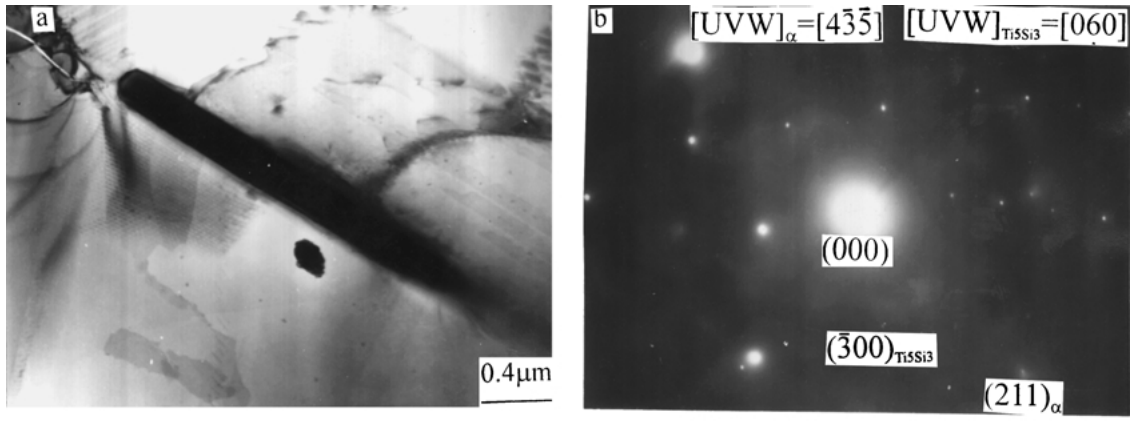

Figure 1 TEM image of A after solution at 910°C for 30 min. (a) rodlike precipitate, (b) indexing of SAD.

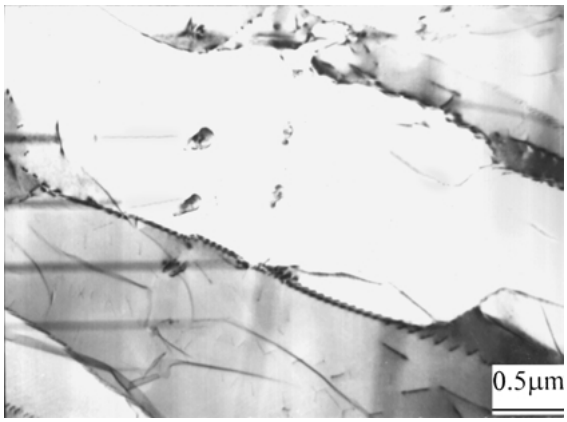

Figure 2 TEM image of A after solution at 750°C for 30 min.

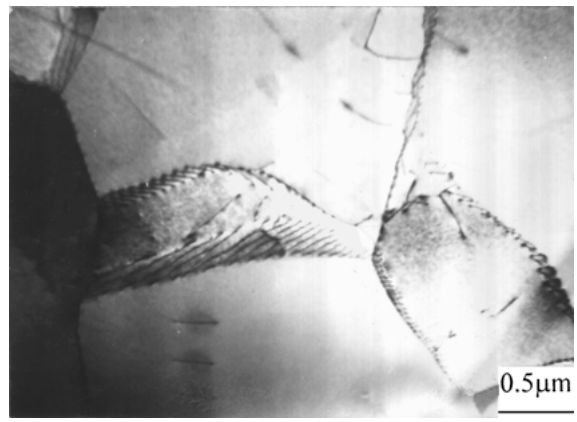

Figure 3 Normal structure of Ti40 alloy solution treated at 910°C.

Fig. 1 shows the TEM image of A after solution at 910°C for 30 min. There are rodlike precipitates of length of 2.2 μm and width of 0.2 μm from the β matrix. The analysis of selected area diffraction (SAD) reveals that they are α and Ti_5Si_3 phases, most being α phase. Micro-crack is induced at the end of the rodlike precipitate. That is, the precipitation of the second phases changes the stress field that leads to stress concentration and micro-crack production.

If solution temperature is below 850°C, such as 750°C, there are not precipitates of second phases. Dislocations arrange regularly along grain boundaries, as shown in Fig. 2. The normal structure of Ti40 alloy solution treated at 910°C is just as that of 750°C solution (Fig. 3), with elongated grains at 750°C. This is that the recrystallization temperature of Ti40 alloy is 800°C [13]. The higher solution temperature, the more second phases (compared Fig. 1 with Fig. 2).

3.1.2. Solution and aging

A new phase, oblique α'' (Fig. 4a) emerges beside α and Ti_5Si_3 phases after A solution at 910°C for 30 min followed by aging at 600°C for 5 h. Acicular structure arranges regularly in the β matrix. The analysis of SAD reveals that it is oblique α'' phase (Fig. 4b). Obvious interface appears between the two group α'' phases. The α'' phases beside the interface arrange crisscrossly along the same direction.

There are no α precipitates after solution at 860°C for 30 min followed by aging at 600°C for 5 h. Only does lath (0.8×0.25 μm) or round-shaped (0.05 μm) Ti_5Si_3 phases precipitate from β matrix (Fig. 5). The dislocations move through Ti_5Si_3 phase.

3.1.3. Exposure at 540°C for 100 h

Fig. 6 shows the TEM images of A exposed at 540°C for 100 h after solution at 910°C for 30 min followed by aging at 560°C for 5 h. Dislocations pile up at round-shaped Ti_5Si_3 phases (Fig. 6a) which retards dislocation movement and induces micro-cracks along grain boundaries or subgrain boundaries (Fig. 6b). In the mean time, there are also α and small size Ti_5Si_3 phases. The existence of α phase further increases the local stress concentration.

Ti_5Si_3 phases precipitate along grain boundaries (Fig. 7) of A exposed at 540°C for 100 h after solution at 820°C for 30 min followed by aging at 600°C for 5 h. There are also Ti_5Si_3 phases within grains (Fig. 7). Ti_5Si_3 phases on grain boundaries reduce the strength of grain boundaries. Fig. 8 shows the TEM images of B exposed at 540°C for 100 h after solution at 820°C for 30 min followed by aging at 600°C for 5 h. There are

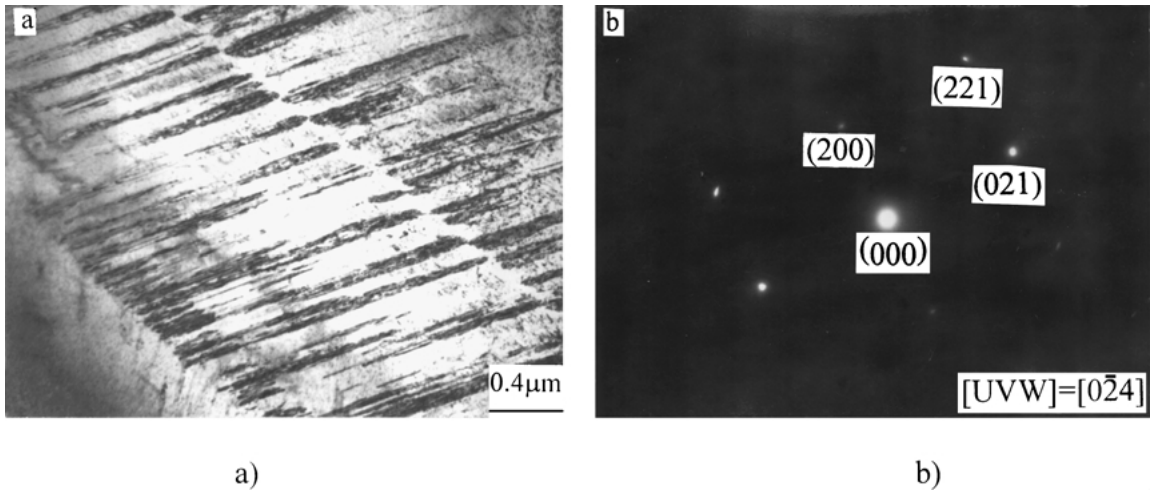

Figure 4 TEM images of A solution at 910°C for 30 min followed by aging at 600°C for 5 h: (a) Oblique α'', (b) indexing of SAD.

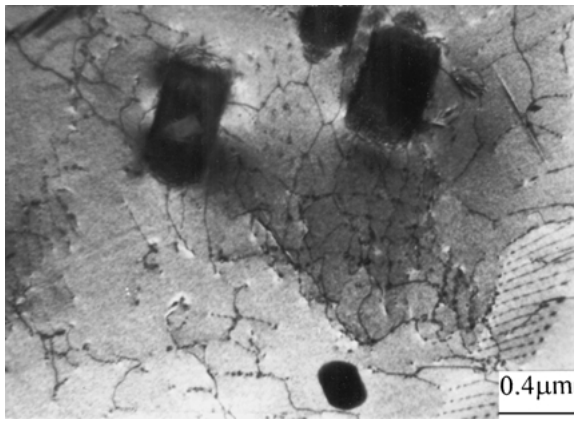

Figure 5 TEM image of A solution at 860°C for 30 min followed by aging at 600°C for 5 h.

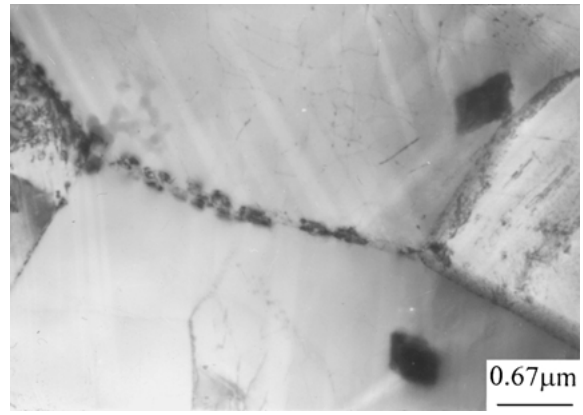

Figure 7 Ti_5Si_3 precipitates along grain boundary and within grains of A exposed at 540°C for 100 h after solution at 820°C for 30 min followed by aging at 600°C for 5 h.

different shape of α and Ti_5Si_3 phases. Round-shaped α or short rodlike α emerges in Fig. 8a, lenticular Ti_5Si_3 phases appear in Fig. 8b, and the precipitates are mainly lath α and blocky α phases in Fig. 8c. There is higher dislocation density around α phases, and the coarse Ti_5Si_3 phases, which indicates that large stress concentration exists around α phases, leading to brittleness.

3.2. Tensile properties and fractographs

3.2.1. Tensile properties at RT and fractographs

Table I shows the tensile properties at RT, and the corresponding microstructures are shown in Figs 4 and 5. The influences of oblique α'', α and Ti_5Si_3 phases within

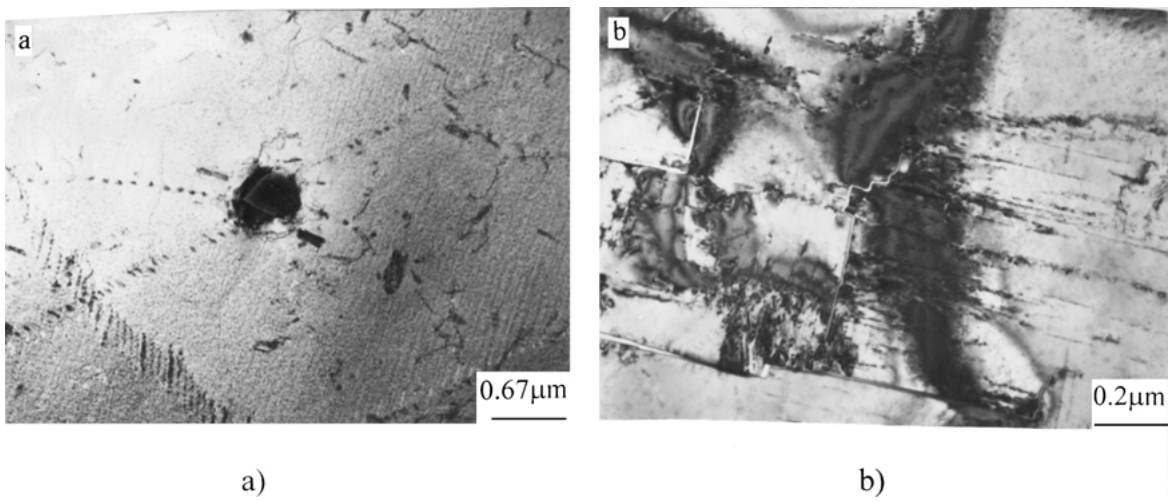

Figure 6 TEM images of A exposed at 540°C for 100 h after solution at 910°C for 30 min followed by aging at 560°C for 5 h: (a) dislocation pile-up at round-shaped Ti_5Si_3 phases, (b) micro-cracks along grain boundaries or sub-grain boundaries.

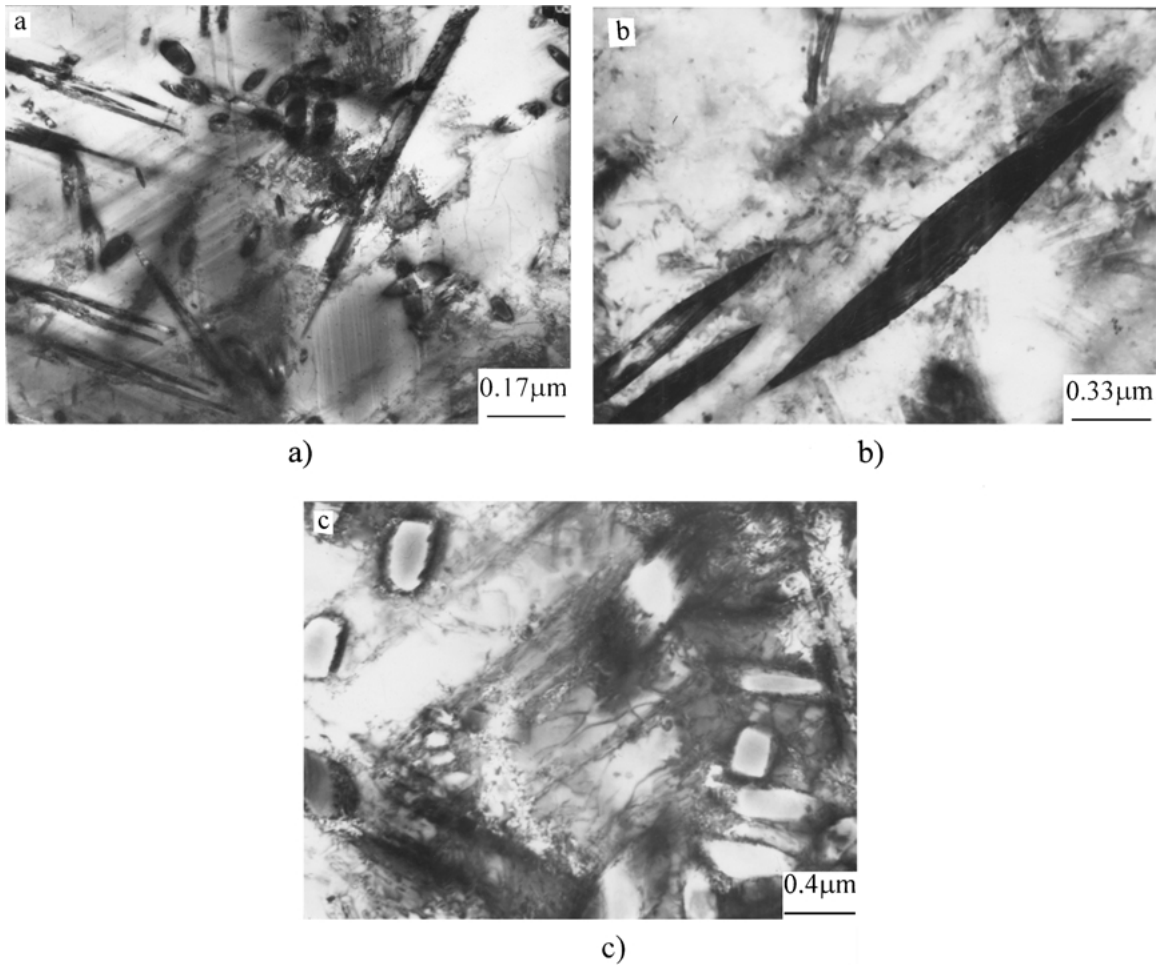

Figure 8 TEM images of B exposed at 540°C for 100 h after solution at 820°C for 30 min followed by aging at 600°C for 5 h: (a) round-shaped α or short rodlike α, (b) lenticular Ti_5Si_3 phase, (c) lath α and blocky α phases.

TABLE I Tensile properties at RT

Heat treatment	UTS (MPa)	YS (MPa)	El. (%)	RA (%)	Second phase
860°C/30 min W.Q +600°C/5 h A.C	979	960	18	30	Lath Ti_5Si_3
910°C/30 min W.Q +600°C/5 h A.C	990	966	24	34	Oblique α'', α and Ti_5Si_3

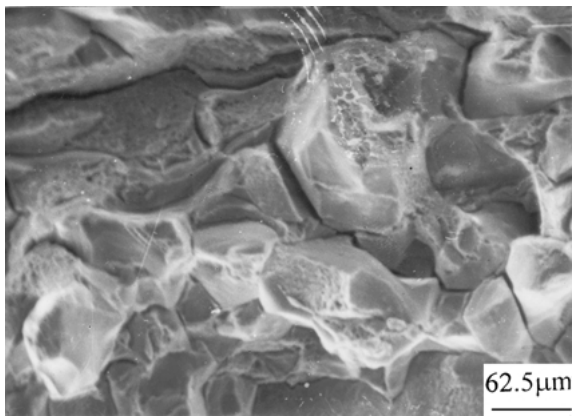

Figure 9 Tensile fractograph of A at RT.

grains on the tensile properties at RT are not obvious. Fig. 9 is the corresponding tensile fractographs. There are deep second cracks and cracks along grain boundaries, which indicates that the grain boundaries are weak and fracture is selectively along the grain boundary. However, many dimples exist within grains, which indicates that the plasticity deformation within grains is significant. During the tensile process, the plasticity deformation within grains controls the fracture behavior, therefore the alloy has high plasticity.

3.2.2. Thermal stability and tensile fractographs

Table II shows the thermal stability of Ti40 alloy after exposure at 540°C for 100 h, and the corresponding microstructures are illustrated in Figs 6, 7 and 8. The precipitation of α phase results in decrease of thermal stability (elongation reduces by 80% and reduction in area reduces by 60%). The increase of α phase volume fraction and coarseness of α further weakens the thermal stability (elongation reduces by 90%). Compared with Table I, the precipitation of Ti_5Si_3 phase along grain boundary weakens the grain boundary, which leads to reduction of thermal stability (elongation decreases from 18% to 9.4%, and reduction in area decreases from 30% to 17%). The synthetical influences of Ti_5Si_3 and α phase further lead to decrease of thermal stability (elongation reduces from 24% to 1.9%, and reduction in area from 34% to 6.3%). The influence of α phases on thermal stability is more obvious than that of Ti_5Si_3 phases.

TABLE II Thermal stability of Ti40 alloy

Heat treatment	UTS (MPa)	YS (MPa)	El (%)	RA (%)	Second phase
820°C/30 min W.Q+ 600°C/5 h A.C, **A**	1077	1007	9.4	17	Ti_5Si_3 along grain boundaries
910°C/30 min W.Q+ 560°C/5 h A.C, **A**	1145	1066	1.9	6.3	Round-shaped Ti_5Si_3 and α
820°C/30 min W.Q+ 600°C/5 h A.C, **B**	917	914	0.2	7	Lenticular Ti_5Si_3 and different α shape

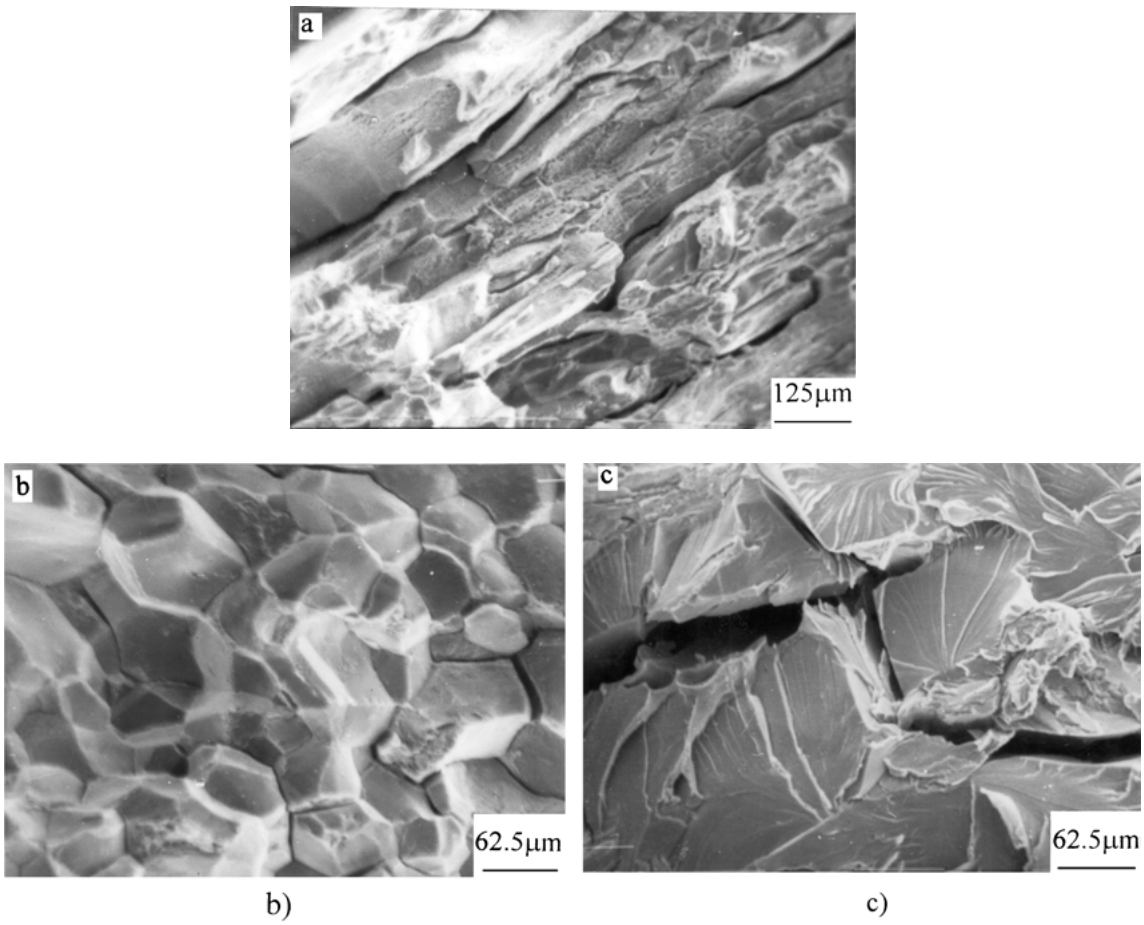

Figure 10 Tensile fractographs after exposure at 540°C for 100 h: (a) A, solution at 820°C for 30 min followed by aging at 600°C for 5 h, (b) A, solution at 910°C for 30 min followed by aging at 560°C for 5 h, (c) B, solution at 820°C for 30 min followed by aging at 600°C for 5 h.

Fig. 10 shows the tensile fractographs of the two heat treatments in Table II. There are obvious intergranular cracks (Fig. 10a) after A solution at 820°C for 30 min followed by aging at 600°C for 5 h, which reveals that the grain boundaries are weak. This is caused by the precipitation of Ti_5Si_3 phases along grain boundary, and the fracture occurs selectively along grain boundary. In the mean time, there are obvious dimples within grains, which suggests large plasticity appears within grains. The deformation within grains has the main influence, which leads to good plasticity. The fracture is obvious brittle transgranular fracture (Fig. 10b) of A exposure at 540°C for 100 h after solution treatment at 910°C for 30 min followed by aging at 560°C for 5 h, which is consistent with its low plasticity. The fracture of B is brittle macro-transgranular fracture with a main crack running through the whole fracture section (Fig. 10c), which is well corresponding with its microstructure and properties.

4. Conclusions

(1) The higher solution temperature, the more second phases in Ti40 alloy. There are not second phases if the solution temperature is below 850°C, while there are rodlike α and little Ti_5Si_3 phases if temperature is over 850°C;

(2) α, Ti_5Si_3 and oblique α'' phases emerge after Ti40 solution at 910°C followed by aging at 600°C, while only Ti_5Si_3 phases emerge after solution at 860°C followed by aging at 600°C. The effect of the second phases on properties at RT are not obvious.

(3) There are different shapes of α and Ti_5Si_3 precipitates after Ti40 alloy exposure at 540°C for 100 h, which decreases the thermal stability.

References

1. S. R. SEAGLE, *Mater. Sci. Eng.* **A213** (1996) 1.
2. R. R. BOYER, *ibid.* **A213** (1996) 103.
3. LOCKHEED MARTIN, *Advanced Mater. Proc.* **59** (1998) 23.

4. UK Patent Application, 2 238057 (1987).
5. Y. Q. ZHAO, X. M. ZHAO and K. Y. ZHU, *Rare Metal Mater. Eng*. **5** (1996) 1.
6. Y. G. LI, P. A. BLENKINSOP and M. H. LORETTO, *Mater. Sci. Technol*. **14** (1998) 732.
7. *Idem*., *Acta Mater*. **16** (1998) 5777.
8. *Idem*., in Proc. 9th World Conference on Titanium, Russia (2000), p. 141.
9. Y. Q. ZHAO, K. Y. ZHU and M. X. ZHAO, Chinese Patent Application, 97 1 12303.9 (1997).
10. Y. Q. ZHAO, L. ZHOU and J. DENG, *Rare Metal Mater. Eng*. **2** (1999) 77.
11. *Idem*., *Mater. Sci. Eng*. **A267** (1999) 167.
12. *Idem*., *J. Alloys Compounds* **284** (1999) 190.
13. Y. Q. ZHAO, K. Y. ZHU and H. L. QU, *Mater. Sci. Eng. A* **316** (2001) 211.
14. K. Y. ZHU, Y. Q. ZHAO and H. L. QU, *J. Mater. Sci*. **35** (2000) 5609.
15. Y. Q. ZHAO, K. Y. ZHU and M. X. ZHAO, Chinese Patent Application, 97 1 12302.0 (1997).
16. Y. Q. ZHAO, Research on Burn Resistant Titanium Alloys—Final Research Report, Northwest Institute for Nonferrous Metal Research, 1996.
17. D. W. ANDERSON and A. F. CONDLIFF, in Proc. of the 10th Annual International Titanium Association Application Conference & Exhibition, 1994, USA, p. 91.
18. A. VASSEL, in "Beta Titanium Alloys in the 1990's" edited by D. Eylon, R. R. Boyer and D. A. Koss (TMS, 1993) p. 173.

Received 27 June 2000
and accepted 24 April 2001